

One promise of polaritonics is the achievement of low-threshold lasing, which does not rely on inversion of the excited state population but on the bosonic nature of the lower polariton state. Instead of needing to scale down the device size (so that inverting all emitters costs less energy), this offers a different paradigm for coherent light emission, using the stimulated scattering of polaritons into their lowest state where they condense into a macroscopic condensate. While a number of polariton lasers have worked with optical pumping, this is unsatisfactory for real devices and a key goal has been incorporating electrical injection into such microcavities.

The combination of high oscillator strength excitons in small optical cavities creates problems for wiring up such devices (Fig. 1). If the electrons overlap the cavity photons, the extra free-carrier absorption often ruins the strong coupling, so that conventional LED structures have to incorporate trade-offs that yield polaritons but no condensation⁷ (Fig. 1a). On the other hand, sideways injection of the electrons has required complex fabrication and highly compromised coupling^{8,9} (Fig. 1b). Even electrical control of the polaritons has been challenging — for instance, in TMD open cavities¹⁰ (Fig. 1c) — though now advanced to the stage where ultra-low-energy switching is possible at low temperatures¹¹. This is where Zaumseil and co-authors show significant progress, using a carbon-based material system not previously considered for polaritonics.

Single-walled carbon nanotubes support tightly-bound, strongly light-emitting excitons at room temperature and around telecommunications wavelengths, but because their energies depend on how the nanotubes roll up, the narrow emission lines required can only be obtained by size-selection. Laying down mats of these nanotubes and electrically contacting from each side allows both electrons and holes to be injected from opposite ends (Fig. 1d). When these recombine in the central zone of a nanotube they form excitons that emit light. A simple planar cavity formed of mirrors above and below the nanotubes reflects the light, giving exciton–photon strong coupling. The one metallic mirror can elegantly be used as a voltage gate that shifts the lateral position of the polariton emission within the microcavity, as well as controlling the polariton energies.

While strong polariton emission is seen in these devices, condensation is not yet observed at high injection currents. A key aspect is the formation of the runaway population of the lower polariton by stimulated scattering from the injected reservoir of hot excitons. Both optical phonons and Coulomb-induced exciton–exciton scatterings contribute, and enhancing the latter is critical. In carbon nanotubes (and other systems with high exciton binding energy), the Bohr radius of excitons is on the nanoscale, with centre of mass delocalization below 100 nm, which reduces the exciton overlap and thus the Coulombic in-scattering. This suggests that high densities will be

required for lasing. Applying vertical fields can polarize the excitons, producing ‘dipolaritons’ (a superposition of a photon and a direct and an indirect exciton) with much larger Coulombic scattering¹² — of great interest in stacked TMD systems, and also potentially of interest in low dimensional systems such as nanotubes. Another promising approach just emerging is the use of plasmonic resonators, which confine light millions of times more tightly than conventional microcavities while retaining polariton splittings exceeding thermal energies⁶. This can strongly enhance the Coulombic scattering and potentially open the way to realistic nonlinear optical devices for optical and quantum processing. □

Jeremy J. Baumberg is at the NanoPhotonics Centre, Cavendish Laboratory, University of Cambridge, Cambridge CB3 0HE, UK.
e-mail: jjb12@cam.ac.uk

References

1. Graf, A. *et al.* *Nat. Mater.* **16**, 911–917 (2017).
2. Christopoulos, S. *et al.* *Phys. Rev. Lett.* **98**, 126405 (2007).
3. Kéna-Cohen, S. & Forrest, S. R. *Nat. Photon.* **4**, 371–375 (2010).
4. Plumhof, J. D., Stöferle, T., Mai, L., Scherf, U. & Mahrt, R. F. *Nat. Mater.* **13**, 247–252 (2014).
5. Liu, X. *et al.* *Nat. Photon.* **9**, 30–34 (2014).
6. Chikkreddy, R. *et al.* *Nature* **535**, 127–130 (2016).
7. Tsintzos, S. I., Pelekanos, N. T., Konstantinidis, G., Hatzopoulos, Z. & Savvidis, P. G. *Nature* **453**, 372–375 (2008).
8. Schneider, C. *et al.* *Nature* **497**, 348–352 (2013).
9. Bhattacharya, P. *et al.* *Phys. Rev. Lett.* **112**, 236802 (2014).
10. Sidler, M. *et al.* *Nat. Phys.* **13**, 255–261 (2017).
11. Dreismann, A. *et al.* *Nat. Mater.* **15**, 1074–1078 (2016).
12. Cristofolini, P. *et al.* *Science* **336**, 704–707 (2012).

Published online: 17 July 2017

RAMAN SPECTROSCOPY

Enhanced by organic surfaces

Nanostructured films of organic semiconductors are now shown to enhance the Raman signal of probe molecules, paving the way to the realization of substrates for Raman spectroscopy with molecular selectivity.

John R. Lombardi

Surface-enhanced Raman spectroscopy (SERS) is a phenomenon in which the normally weak Raman signal of a molecule is strongly enhanced by proximity to a nanostructured surface. Most of the early work on this topic utilized silver as a substrate, as this metal resulted in the largest observed enhancement factors^{1,2} — up to 10^{12} — enabling the detection of a single molecule^{3,4}. In fact, one of the most promising applications of this spectroscopic

technique is its use in ultra-sensitive qualitative analytic tools for the detection and identification of trace quantities of a molecular species. In order for this to be realized, a SERS substrate must be found that is inexpensive, reproducible, stable, robust and, if possible, reusable. Substrates constructed from silver and other coinage metals have not been found to fit all these criteria, so there have been attempts to find alternative substrates, including the

possibility of semiconductor substrates. Writing in *Nature Materials*, Mehmet Yilmaz and colleagues⁵ now demonstrate that organic semiconductors, either pristine or in combination with thin metal coatings, represent a previously unexplored platform for the realization of high-performing SERS-based sensors.

Crucial to the Raman enhancement on metal substrates is the existence of a plasmon resonance. Plasmons are generated

when an electromagnetic wave excites the electrons in the conduction band of the metal to collective and in-phase motion, oscillating at the optical frequency of the exciting laser. This results in a very high electric field on the nanoparticle surface, which leads to a strongly augmented Raman signal from the adsorbed molecule. In addition, other resonances in the molecule–metal system also contribute to the enhancement; namely, a charge-transfer resonance between the metal Fermi level and an empty orbital on the molecule, or the reverse transition between a filled orbital in the molecule to the Fermi level of the metal. Further enhancements are observed when a molecular resonance is in the vicinity of the laser frequency. All these resonances are combined in a unified manner, contributing multiplicatively, and coupled by a vibronic expression⁶ that enables the prediction of the changes in the observed Raman spectrum due to the interaction of the molecule with the surface. The mechanism of enhancement can then be attributed to the increase of the (normally weak) charge-transfer intensity due to intensity ‘borrowing’ from a nearby allowed optical transition⁷.

When semiconducting nanostructured films or nanoparticles are used instead of metals as substrates, lower enhancement factors are expected due to lack of plasmon resonances in the conduction band of the semiconductor. However, additional resonances could be harnessed due to Mie scattering resonances that depend on the nanostructures’ shape and/or exciton (band gap) resonances in semiconductor nanoparticles. These resonances can also couple vibronically with charge-transfer and molecular resonances⁸ to produce larger SERS enhancements. Compared to metal enhancements, these were rather weak at first, typically on the order of 10^3 or 10^4 . However, by taking advantage of improvements in the synthesis of inorganic semiconductor nanoparticles, higher enhancements (10^5 – 10^6) have been obtained^{9–11}.

Yilmaz and co-workers now extend SERS to an entirely new realm of organic semiconductor substrates. The researchers utilized a π -conjugated organic substrate composed of α,ω -diperfluorohexylquaterthiophene (DFH-4T) to form a thin nanostructured film (Fig. 1a). This consisted of vertically aligned two-dimensional nanoplates connected to a cylindrical central spine. The dyes methylene blue (MB) and rhodamine 6G (R6G) were chosen for the probe molecules, and the excitation energy was 1.58 eV (wavelength 785 nm). For MB, they found an enhancement factor of over 10^3 . By depositing a thin layer of Au over the DFH-4T before

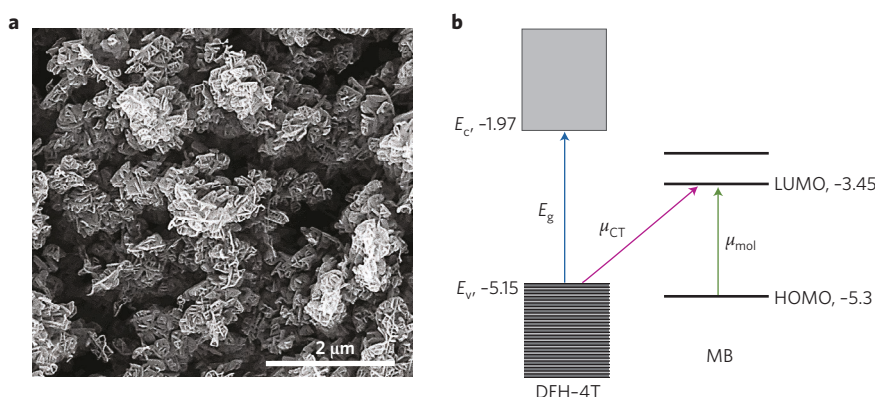


Figure 1 | Mechanisms for the enhancement of the Raman signal due to the interaction of a molecule with a semiconductor substrate. **a**, Scanning electron microscopy image of the nanostructured organic films used by Yilmaz and colleagues⁵. **b**, Enhancement of MB Raman signal in proximity of an organic semiconductor substrate (DFH-4T). The charge-transfer transition μ_{CT} between the edge of the valence band E_v of DFH-4T and the LUMO level of MB is marked with a red arrow, and the molecular transition μ_{mol} between the HOMO and LUMO levels of MB is marked with a green arrow. These transitions are close to each other spectroscopically and coupled to produce the Raman enhancement. The exciton transition E_g between E_v and the edge of the conduction band E_c in the semiconductor, shown in blue, lies too far away to contribute significantly to the enhancement. Numbers represent the energy values in eV as measured from the vacuum (0.0 eV). Panel **a** reproduced from ref. 5, Macmillan Publishers Ltd.

adding the molecule, enhancement factors of up to 10^{10} were obtained, illustrating the possible contribution of a plasmon resonance. The experimental observations, further supported by density functional calculations, showed that the enhancement of the pristine organic film is due to a charge-transfer transition between the molecule and the organic substrate (Fig. 1b). This interpretation is consistent with the resonance description of SERS in that the charge-transfer resonance (around 1.58 eV) between molecule and substrate is vibronically coupled to the nearby molecular transition and borrows intensity from it. In MB, the molecular transition is at 1.85 eV (668 nm), close enough to the experimental charge-transfer transition to provide additional enhancement through intensity borrowing. On the contrary, changing the substrate to DH-4T (unfluorinated substrate) moves the charge-transfer resonance farther away from the excitation energy, severely lowering the observed enhancement. Changing the analyte to R6G has a similar effect. These observations also emphasize the importance of structural features of the substrate in explaining the observed effect.

Why should we be so encouraged by the promise of organic semiconductors for SERS substrates? In this application, it has been shown that nanostructured semiconductor films are generally more stable and reproducible than their metallic counterparts. Another advantage is the ability to tailor the properties of the semiconductor to a

specific molecule or class of molecules. The coinage metals are more of a universal substrate, effective with almost any molecule for which the Fermi level of the metal lies between the highest occupied molecular orbital (HOMO) and the lowest unoccupied molecular orbital (LUMO). This facilitates charge transfer that, coupled to the plasmon resonance, produces high enhancements. In contrast, charge transfer between a molecule and a semiconductor substrate involves the semiconductor band edges, rather than its Fermi level. This provides an advantage over metallic substrates, because the band edge of a semiconductor can be easily tailored to optimize the charge transfer to a particular molecule⁸. Since many real-life samples come as mixtures, the appropriate semiconductor can act as a selective detector for a specific molecule in that mixture. Organic semiconductors can further this selectivity, since we often have chemical control of the exact location of the band edges. For example, by adjusting the number of thiophene rings in the central chain of DFH-4T (for instance, to DFH-5T), or by replacing the fluorines with hydrogen (such as with DH-4T), we can finely tune the location of the band edges, providing more precise control over the location of charge-transfer transitions to and from a specific molecule to be detected. The results of Yilmaz and colleagues have the potential to open up a whole new area of research. Considerable work has been carried out on the optical properties of many other organic semiconductor systems, which, with

proper integration with theory, can vastly expand the applicability of SERS to the field of molecular sensors. □

John R. Lombardi is in the Department of Chemistry, City College of New York, 138th Street at Convent Avenue New York, New York 10031, USA. e-mail: jlombardi@ccny.cuny.edu

References

1. Fleischmann, M., Hendra, P. J. & McQuillan, A. *J. Chem. Phys. Lett.* **26**, 163–166 (1974).
2. Jeanmaire, D. L. L. & Van Duyne, R. P. *J. Electroanal. Chem. Interfacial Electrochem.* **84**, 1–20 (1977).
3. Nie, S. & Emory, S. R. *Science* **275**, 1102–1106 (1997).
4. Kneipp, K. *et al.* *Phys. Rev. Lett.* **78**, 1667–1670 (1996).
5. Yilmaz, M. *et al.* *Nat. Mater.* **16**, 919–924 (2017).
6. Lombardi, J. R. & Birke, R. L. *J. Phys. Chem. C* **112**, 5605–5617 (2008).
7. Albrecht, A. C. *J. Chem. Phys.* **34**, 1476–1484 (1961).
8. Lombardi, J. R. & Birke, R. L. *J. Phys. Chem. C* **118**, 11120–11130 (2014).
9. Maznichenko, D., Venkatakrishnan, K. & Tan, B. *J. Phys. Chem. C* **117**, 578–583 (2013).
10. Li, W. *et al.* *J. Am. Chem. Soc.* **135**, 7098–7101 (2013).
11. Islam, S. K., Tamargo, M., Moug, R. & Lombardi, J. R. *J. Phys. Chem. C* **117**, 23372 (2013).

Published online: 7 August

MICROPOROUS POLYMERS

Ultrapermeable membranes

Microporous membranes were designed from the loose packing of two-dimensional polymer chains — a breakthrough giving both ultrahigh permeability and good selectivity for gas separations.

Yan Yin and Michael D. Guiver

Membrane technology is displacing established molecular-separation processes by avoiding energy-intensive phase changes, achieving higher efficiency at lower cost. Industrial membrane gas separation began in the 1980s and the dominant separations are currently N_2 production from air, CO_2 removal from natural gas, and H_2 recovery from various industrial process streams¹.

In polymeric membranes, gas transport occurs by the solution–diffusion mechanism, whereby gases sorb and then permeate by pressure differential through voids (fractional free volume, FFV) created by intermolecular gaps between polymer chains. Highly rigid polymer chains allow selective permeation of gases with smaller kinetic diameters (for example, H_2) over larger kinetic diameters (for example, N_2).

Condensable gases such as CO_2 achieve additionally higher permeability through gas sorption interactions with the polymer. Higher gas permeability often comes with lower selectivity, and this performance trade-off was initially defined in 1991 by the Robeson upper-bound plots (log permeability of faster gas versus log selectivity of specified gas pair)². The development of polymers of intrinsic microporosity (PIMs)³ in 2008 pushed the upper bounds higher⁴. Now, writing in *Nature Materials*, Ian Rose and colleagues⁵ report a PIM membrane with both ultrapermeability and superior selectivity, launching a new chapter in the design of PIMs for high-performance membrane gas separation.

Microporous materials are materials with interconnected pores less than 2 nm in diameter, comparable to molecular diameters⁶. In the membrane field, poly(trimethylsilyl-1-propyne) (PTMSP) has long been established as an ultrapermeable microporous polymer, with the highest known gas permeability⁷. This ultrapermeability derives from very large FFV and restricted chain mobility, attributable to a rigid alternating double-bond backbone substituted with trimethylsilyl groups. For example, CO_2 permeability is 20,000–30,000 barrer, several orders of magnitude higher than other polymeric membranes. However, very low gas selectivity and the propensity for free-volume collapse hinders applications.

PIMs were invented by Peter Budd and Neil McKeown³, and are characterized as having rigid, ladder-like chains connected to contortion sites, giving twisted macromolecular structures with

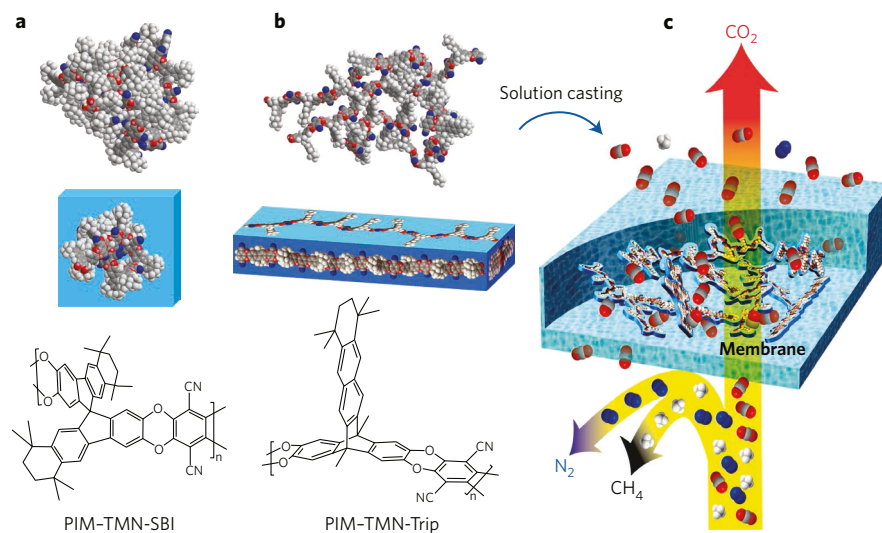


Figure 1 | Representation of the PIM-TMN-Trip membrane, and comparison of chemical structure and polymer packing of 2D and 3D PIMs. **a**, The 3D chain packing of PIM-TMN-SBI, a contorted polymer with primarily smaller micropores, thus giving lower gas permeability than the PIM-TMN-Trip membrane. **b**, The chemical structure of ribbon-like 2D polymer PIM-TMN-Trip, and energy-minimized chain packing. The polymer generates 3D amorphous molecular sieve-like solids with additional intrinsic microporosity, arising from the coexistence of larger micropores (giving ultrapermeability) and smaller micropores (which enhance selectivity). **c**, Schematic of PIM-TMN-Trip membrane, which allows unprecedented ultrapermeability of gases such as CO_2 through the membrane, while simultaneously maintaining good selectivity against gases with larger kinetic diameter such as N_2 and CH_4 .